Journal of Materials Science and Engineering B 4 (12) (2014) 337-345
doi: 10.17265/2161-6221/2014.12.001

Enhanced Steam Condensation on Meso- and Micro-scale Profiled Surfaces

Axel Kölling[1], Stefan Kohn[2], Mario Nowitzki[2], Udo Hellwig[3] and Nikolai Sachno[3]

1. Research and Development, ERK Eckrohrkessel GmbH, Berlin 12435, Germany

2. Process Engineering, University of Applied Sciences Wildau, Wildau 15745, Germany

3. Research and Development, La Mont GmbH, Wildau 15745, Germany

Received: November 12, 2014 / Accepted: December 04, 2014 / Published: December 25, 2014.

Abstract: Depending on their specific surface energy transition metals like copper, nickel and their alloys are appropriate to induce dropwise condensation, in particular of water steam on sub-cooled micro-scale profiled surfaces. Special tube probes made of alloyed steel No. 1.4301 with meso-scale profiled surface, micro-scale profiled probes and combined meso- and micro-scale profiled probes made of copper No. 2.0090 were designed, prepared and studied. The principal result is that drop condensation was induced successfully and a significant increase in heat flux density by at least 80% was obtained. This is correlated with augmented heat transmittance, condensate formation and the mass flow of the cooling fluid quantified by the Reynolds number. It could be transferred effectively to a newly constructed prototypic water steam condenser, evaluated by experiment and by modelling using methods of numerical calculation (CFD). Inherently, the micro-scale profiled surfaces cause an increase in the surface tension of the fluid as indicated by contact angle measurements. Further investigation is necessary regarding special meso-, micro- and nano-scale profiled surfaces potentially with additional substantial coatings or artificially prepared compound substrates and textured composites to adjust the specific surface properties, thereby achieving the ability to induce enhanced condensation of a wide range of polar, non-polar and olefin substances in energy and process technology.

Key words: Transition metal, induced dropwise condensation, heat flux density, heat transmittance.

Nomenclature

a: Temperature conductivity
A_A: Outer surface area of the tube
A_I: Inner surface area of the tube
bt_s: Depth of meso-scale profile
c_{pL}: Heat capacity of the fluid
d_A: Outer diameter of the tube
d_{Hyd}: Hydraulic diameter of the tube
d_I: Inner diameter of the tube
g: Gravitational acceleration
Δh_V: Enthalpy of condensation
H: Characteristic length of condensate film
k: Heat transmittance
L: Tube length
$\dot{m}$: Mass flow
n: Number of tube rows of a bundle
s: Wall thickness
Re: Reynolds number
Pr: Prandtl number
Nu: Nusselt number
p: Pressure drop
Q: Heat flux
$\dot{Q}$: Heat flux density
T_S: Steam temperature
T_w: Wall temperature
T: Sub-cooling temperature difference
t_{log}: Algebraic number of temperature difference relation
v: Velocity
x: Length of condensate film flow

Greek Letters

α_α: Outer heat transfer coefficient
α_i: Inner heat transfer
α_x: Local heat transfer coefficient

Corresponding author: Axel Kölling, doctor, manager R & D, associate professor, research fields: particle physics, and thermodynamics. E-mail: akoelling@eckrohrkessel.com.

$\bar{\alpha}$: Average heat transfer cofficient
$\bar{\alpha}_w$: Average horizontal heat transfer coefficient
$\bar{\alpha}_T$: Average heat transfer coefficient of *n* tube rows
$\bar{\alpha}_n$: Average heat transfer coefficient of *n* tube rows
δ: Thickness of condensate film
λ_L: Heat conductivity of condensate film
λ: Heat conductivity of tube wall
η_L: Dynamic viscosity of condensate film
ρ_L: Density of condensate film
ρ_G: Density of gas phase
ξ: Fluid flow resistance of tube
ν: Kinematic viscosity

1. Introduction

In reference of enhancing the heat transfer in energy and process technology significantly, it is appropriate to induce dropwise condensation, in particular of water steam on sub-cooled surfaces. Usually the induction is achieved by adding vaccines (alcohols, etc.) to the steam or putting promoters (waxes, etc.) on the surface to inhibit wetting partially, thereby disrupting the condensate film resistance and gaining an order of magnitude higher heat transfer [1-4]. Of course, these chemicals are expended during the operation of the condenser, wherefore one would quest for a more durable solution. In principal, there is a wide range of methods for the preparation of the condenser surface with the aim to induce dropwise condensation and achieve increased heat and mass transfer. In general, there are a huge number of chemical techniques, e.g., coatings and self-assembling molecules, as well as physical techniques, e.g., coatings, textures and profiles [5]. Depending on the specific surface energy transition metals like copper, nickel and their alloys work well, whilst steel and the semi-metal aluminum seem to be less effective [6, 7]. Micro-scale profiles seem to influence the surface tension of the fluid and thereby the interfacial tension between vapour, fluid and solid, which determine the process, while the type and geometry of the profile allows to justify the character of the surface in a wide range between superomniphobicity and superomniphilicity [8].

At present, even artificially prepared compound substrates, textured composites and especially monolithic solid plates and tubes with meso-, micro- and even nano-scale profiled surfaces are prepared and tested [9]. A brief literature review showed that up to now, the surface preparation techniques are categorized on the one hand to be top down (vapor deposition, lithography, etching, etc.) or bottom up (growth, oxidation, etc.) and on the other hand, as chemical (polymers, carbon tetrachlorid, polytetrafluoroethylene, self-assembling molecules, etc.) or physical (noble metals, ions, silicon and silicon-finished copper substates prepared by micro-electrical-mechanical structuring and coating, ceramics, ribs, fins, etc.), summarily [10-17]. Furthermore, some details were studied by experiment and simulation, e.g., the contact angle, drop formation and coalescence [18-20].

Therefore, significant contributions based on this approach could be expected in the development of new materials for energy and process technology. Regarding the ongoing work on dropwise and film condensation of water steam enhanced efficiency, effectiveness and specificity were detected and will be reported in the following.

2. Experiments

Sets of meso-scale, micro-scale and both meso- and micro-scale profiled copper and steel tubes with bt_s/d_{Hyd} = 0.02-0.15 and 1,000-3,300,000 straight pins and a prototypic water steam condenser were designed, fabricated, built and investigated during steam condensation experiments and by modelling applying procedures of numerical calculation (CFD) realized with an open source software and commercial software (Figs. 1-3). Complementary experiments and investigations were carried out using physical and chemical methods as well as scanning electron microscopy techniques.

Tube probes were manufactured of steel No. 1.4301 or ASTM A213 in the cases of meso-scaled profiles and copper No. CW024A or 2.0090 in all other cases, especially the meso- and micro-scale profiled tubes.

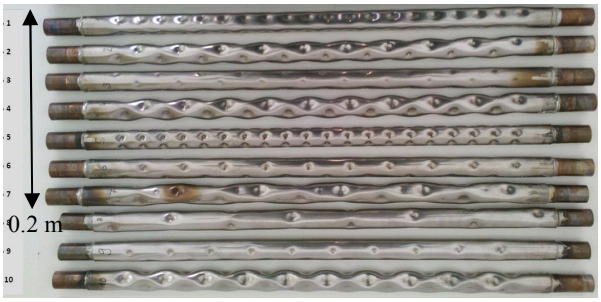

Fig. 1 Meso-scale profiled tube probes.

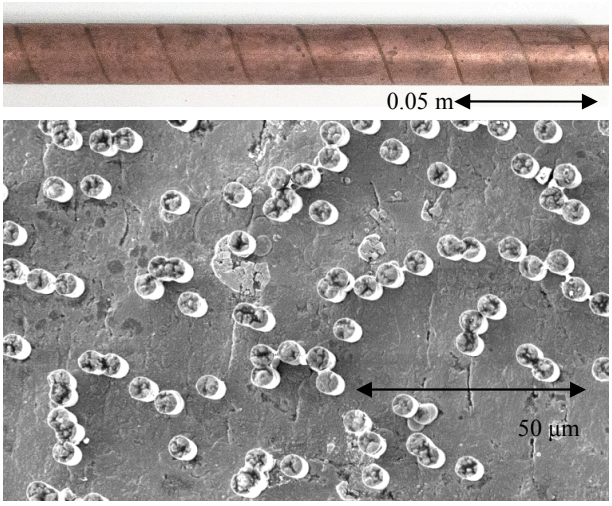

Fig. 2 Straight pins on a micro-scale profiled tube probe.

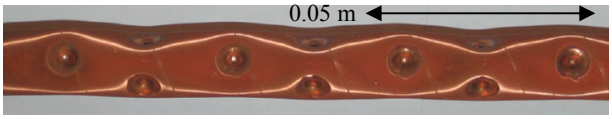

Fig. 3 Meso- and micro-scale profiled tube probe.

The steel tubes were fabricated physically top down by means of a forming machine consisting of a radial propulsion tool and definite sets of exchangeable pressure parts with different geometries (Fig. 1). The copper tubes were covered with a polycarbonate foil physically perforated by argon ion spur techniques top down and subsequently chemically treated bottom up by galvanic deposition and etching processes resulting in so called micro- or nano-pins (Fig. 2). The combined meso- and micro-scaled profiles were generated by a synthesized procedure (Fig. 3). More details are published elsewhere [21].

The experiments were performed applying evaporation, condensation and electric control circuits (Fig. 4). The evaporation circuit consisted of an evaporator with a feed water vessel and a condenser, each specifically designed for the experiments. Except the condenser and the annular gap steel tube cooler made of steel Nr. 1.4301 or ASTM A213, all of the components were standard devices.

The evaporator was made of steel No. 1.0254 or ASTM A53 with hot-dip galvanized interior. The heating power was achieved by six equal heating rods model Redring RS4676819 and amounted 18 kW.

The condenser was built of borosilicate glass Boro 3.3, substantially and thermally isolated by a protective copper No. CW004A or UNS C11000 covering with an inserted 2.5 square inch observation window. Two different steel tube end pieces were used, one pair for the investigation of single tubes and the other one for a tube bundle consisting of four

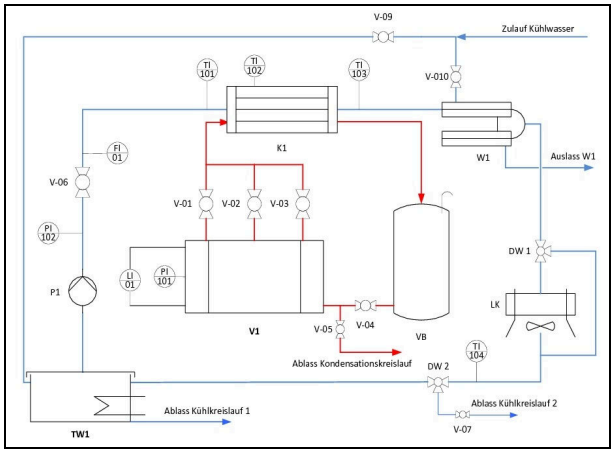

(a)

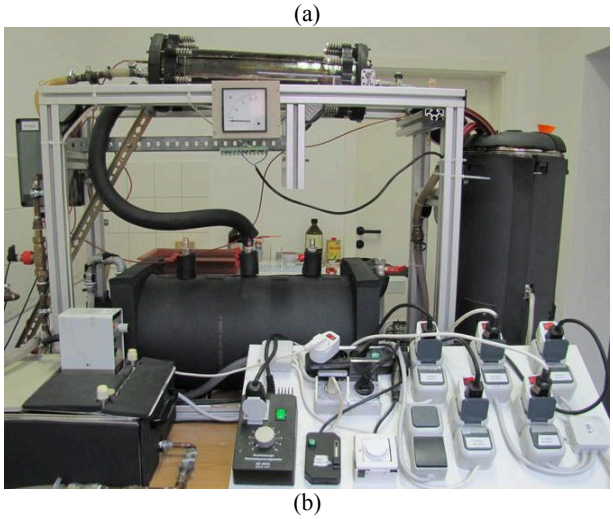

(b)

Fig. 4 (a) Process and control diagram and (b) experimental set-up with evaporator and condenser.

identical objects. Temperature measurements were carried out using Ahlborn FPA32L0100 + OPG5 Pt100 thermocouples with a range of 73.75 to 673.15 K and an accuracy of ±0.16 K.

The cooling circuit was constructed of the condenser on the liquid side, the air cooler, an annular gap tube cooler with aluminum fittings, thermostat, float-type flow meter and a frequency converter. As air cooler, the type of a water-cooled LUVE Contardo SHVN 15/6 S 9811 with 14 kW power was used. For the adjustment of the three-phase Linn T65E cooling water pump with a capacity of 0.834 liter per second, a Peter electronic frequency converter FUS 150/E2/IP65 was operated. The thermostat was a Haake D1, the float-type flow meter an axial-turbine Ahlborn FV A915 VTH K(M) with a range of 0.034 to 0.67 l s^{-1} and an accuracy of ±1%. The registration of the measured values was carried out with an Ahlborn MA85909 data logger, additional observations were made by video recording and photography.

The calibration of the experimental set-up was realized according to the water film theory of Nusselt. On the basis of some simplifying, but sound assumptions concerning a viscous condensate film flow on a horizontally arranged tube, the heat transfer coefficient can be expressed by:

$$\bar{\alpha}_{waag} = 0.728\left[\frac{\rho_L\left(\rho_L - \rho_G\right) g\Delta h_V \lambda_L^{\,3}}{\eta_L\left(T_S - T_W\right)}\frac{1}{d}\right]^{1/4} \quad (1)$$

In it, all of the substance specific values were averaged and applied to the wall temperature and the boiling temperature of the condensate. The value in the vertical case is about one quarter greater.

For a turbulent condensate film flow, the semi-empirical formula of the heat transfer coefficient, which depends on the degree of the sub-cooling temperature difference, is quantified by:

$$\bar{\alpha}_T\left(T_S - T_W\right) = \frac{H \cdot \dot{m}}{A} \quad (2)$$

Taking the generalized equation of heat transfer the heat transmittance k_A with the relations of system specific surfaces, a material specific quotient and α_A the heat transfer coefficient in Eq. (1) is equal to:

$$\frac{1}{k_A} = \frac{1}{\alpha_I} \cdot \frac{A_A}{A_i} + \frac{s}{\lambda} \cdot \frac{A_A}{A_M} + \frac{1}{\alpha_A} \quad (3)$$

Taking the cooling fluid as the basis, k_A can be measured directly using a relation of the heat flux, the surface area and an algebraic expression of the temperature difference:

$$k_A = \frac{Q}{\Delta T_{log} \cdot A_A} \quad (4)$$

To estimate the inner heat transfer coefficient α_i, the Gnielinski-Model was used:

$$Nu = \frac{\left(\frac{\xi}{8}\right) Re \cdot Pr}{1+12.7\sqrt{\frac{\xi}{8}}\left(Pr^{\frac{2}{3}}-1\right)}\left[1+\left(\frac{d_i}{L}\right)\right]^{\frac{2}{3}}\left(\frac{Pr}{Pr_W}\right)^{0.11} \quad (5)$$

The friction resistance coefficient ξ of the tube wall is given by a model of Prandtl und Karmann:

$$\xi = \left(1.8\log_{10} Re\text{-}1.5\right)^{-2} \quad (6)$$

In cases of turbulent flow, the relation of Dittus-Boelter can be applied:

$$Nu = C \cdot Re^{\mathrm{m}} \cdot Pr^{\mathrm{n}} \quad (7)$$

The Nusselt number is equal to:

$$Nu = \frac{\alpha_i \cdot d_{Hyd}}{\lambda} \quad (8)$$

The Reynolds number is estimated by:

$$Re = \left(\frac{\vec{v} \cdot d_{Hyd}}{v}\right) \quad (9)$$

The Prandtl number is quantified by:

$$Pr = \left(\frac{v}{a}\right) \quad (10)$$

Taking the effective wall temperature T = 369.76 K, the heat transfer coefficient on the condensate side was estimated to be α_A = 16,353 $W \cdot m^{-2} \cdot K^{-1}$, which is quite well according to the value obtained by Eq. (1).

3. Experimental Results

In any case, the sub-cooling temperature difference

was varied in equidistant intervals of ΔT = 5 K in the range between 10 and 70 K at a pressure of p = 1.1 bar. In the same way, the Reynolds number Re of the cooling fluid flow was parametrized in intervals of Re = 5,000 between 5,000 and 25,000 in reference of the sub-cooling temperature difference of ΔT = 60 K.

Each type of tube probe showed an increased condensation rate compared to the plain tubes, but in different specific characteristics (Figs. 5, 6, 8 and 12).

With respect to the meso-scale profiled tube probes, notwithstanding whether single or a bundle, the heat flux density increases with increasing sub-cooling temperature difference and appears to be enhanced by 80% in comparison to the plain tube probe. Probably there is no measurable condensation resistance, because no threshold value of the sub-cooling temperature difference could be detected. The slope of the function might well be of the type of a potential function consisting of characteristic parameters of the experimental set-up, specific material constants and the indicated variables. The regression analysis according to Newtonian least square fit method in any case yielded a measure of determination larger than R^2 = 0.98, corresponding to the proportional variance.

Focusing the heat transfer process from the condensate side to the cooling medium, the main physical barrier consists of the thin wall near boundary layer limiting the inner heat transfer coefficient α_i. By means of the meso-scaled profiles with geometry parameters in the range of bt_s/d_{Hyd} = 0.02-0.15, this limitation is significantly reduced so that a larger heat flux density is achieved.

In virtual experiments, the local heat transfer coefficient α_i at the interior wall of the tubes was investigated taking into account a sub-cooling temperature difference of ΔT = 60 K at a pressure of 1.1 bar. Using k-ω-SST-model in computational fluid dynamics a maximal value of α_i = 11.4 kW·m^{-2}·K^{-1} was obtained, whereas the average equals approximately α_i = 3.5 kW·m^{-2}·K^{-1} (Fig. 7). These results are similar to those found in literature for copper and steel sheet and tube surfaces without and with promoters [7, 10, 14].

In terms of the micro-scale profiled tube probes, the effects turned out to be completely different. Drop condensation with drop diameters of 0.0005-0.003 m was induced successfully on the surface (Fig. 9). Up to a threshold value of about ΔT = 30 K, there was no

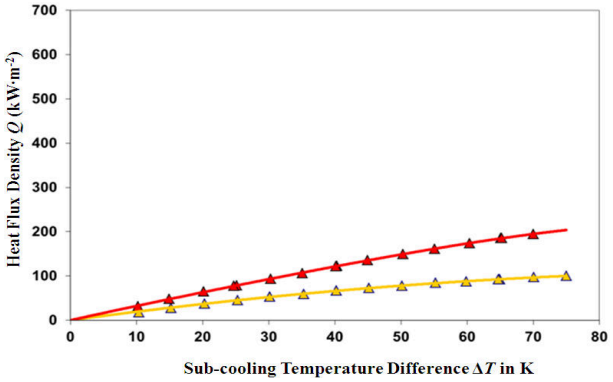

Fig. 5 Variation of heat flux density with sub-cooling temperature difference of film condensation on meso-scale profiled (▲) and plain tube (△).

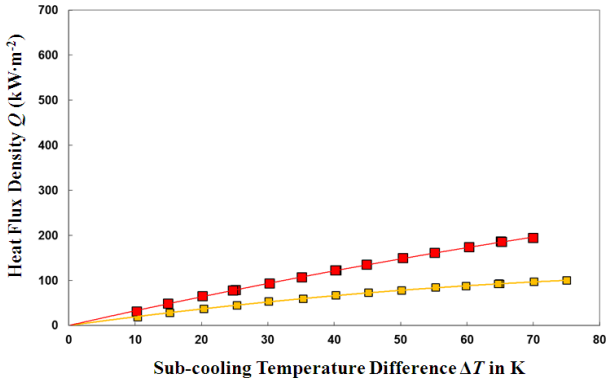

Fig. 6 Variation of heat flux density with sub-cooling temperature difference of film condensation on meso-scale profiled (■) and plain tube bundle (■).

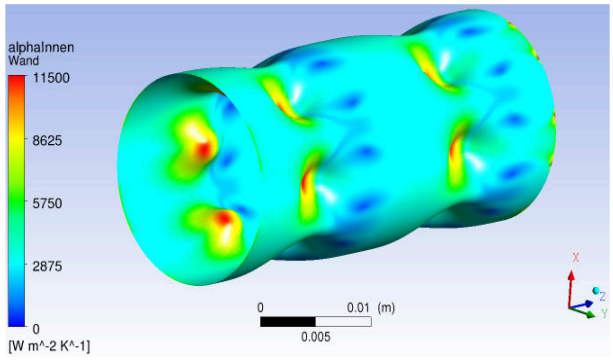

Fig. 7 Contour of the heat transfer coefficient α_i of the inner surface of the meso-scale profiled tube.

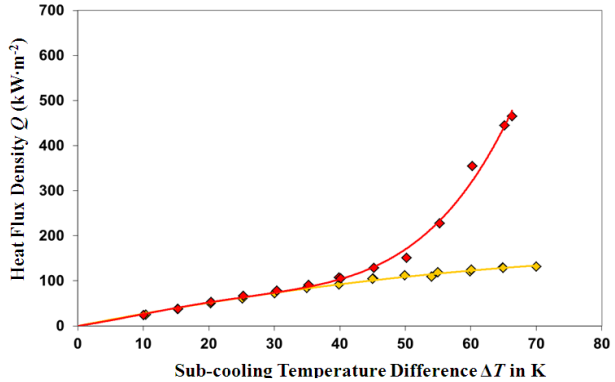

Fig. 8 Variation of heat flux density with sub-cooling temperature difference of drop condensation on mirco-scale profiled (◆) and plain tube (◇).

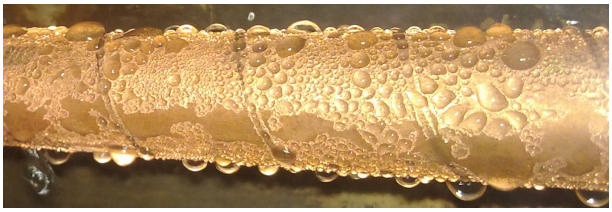

Fig. 9 Induced dropwise condensation on a horizontally arranged micro-scale profiled copper tube.

difference between the sorts of probes and the slope of the function seems to be of the type of a potential function (Fig. 8). Therefore, it is supposed that a kind of condensation resistance has an effect on the measured heat flux density analogous to that occurring in nucleate pool boiling at low heat flux densities. At sub-cooling temperatures larger than $\Delta T \geq 30$ K, in particular the heat flux density of the micro-scale profiled tube bearing 1,000 pins per square centimeter was increased accumulatively up to a factor of 3.9 at $\Delta T = 65$ K compared to the referential one and had a value of 470 kW·m^{-2}, thereby outrunning the thermal capacity of the evaporator. In this region, the slope of the function appears as the type of an exponential function. Compared to the ferrous metal, the heat flux density of the plain copper tube at $\Delta T = 30$ K appears to be increased by 45%, while the heat conductivity is a factor of twenty as large.

By video recording, a sequence of 30 pictures was taken within 45 seconds which clearly shows the coalescence of condensed drops (Fig. 10). On the left hand in Fig. 9, there is a drop stripping off the surface underneath the horizontally fixed micro-scale profiled copper tube probe.

In addition, orientating measurements of the contact angle of water on planar copper surfaces arranged horizontally at room temperature $T = 293$ K and 1 bar pressure were made. Compared to the plain probe, the contact angle on the micro-scale profiled one with a characteristic length of 1 μm was obviously increased by 80% and has a value of about 75°, indicating that the interface surface tension is slightly increased (Fig. 11) [22]. Although the surface tension decreases by roughly a factor of two at about 373 K, the specific effect of the pins would be conserved.

Heterogeneous condensation of water steam would require approximately 10^5-10^8 nucleation sites per square centimeter, for which the edges of the pins could be propitious as an initial vector [23]. However, the condensation process is of stochastic character with low rates, only if the sub-cooling temperature ΔT exceeds the threshold value of 30 K, it becomes snowballed increasing. By the time, the micro drops grow by direct homogeneous condensation from the steam and by coalescence on the material (Fig. 10).

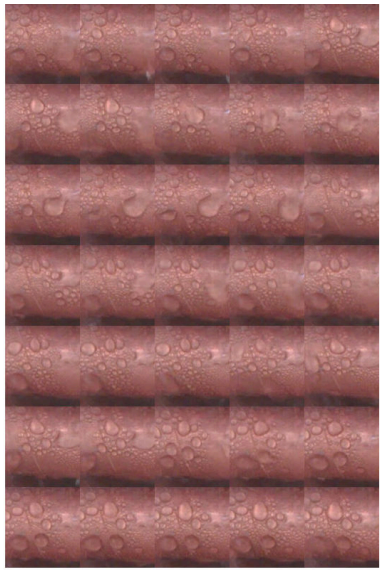

Fig. 10 Coalescence of droplets in a sequence with $\Delta t = 1.5$ s.

Fig. 11 Planar micro-scale profiled surface, contact angle on a plain and a micro-scale profiled plate.

Comparatively, copper is qualified as reasonable hydrophilic like aluminum, for example, wherefore water could condense and adhere to the surface in the form of water droplets [24]. A specific profiling of the surface on the micro-scale makes it possible to tune the grade of hydrophilicity, demonstrated by the experiment at room temperature, as well as that of hydrophobicity. Thereby the surface area covered by drops should be decreased compared to a plain material, while the heat flux transferred would be increased.

In the case of meso- and micro-scale profiled copper tube probes, an increased heat flux density by a factor of 3.5 was observed and the maximal value of the heat flux density was equal to 400 kW·m^{-2} (Fig. 12). The slope of the function seems to be similar than that of the meso-scale profiled tube probes and of the type of a potential function, but the gradient is much larger. Additionally, it cannot be a mere superposition of the functions of the meso- and micro-scale profiled tube probes, because even at a low subcooling temperature difference ΔT = 10 K, the heat flux density is increased by a factor of 3 with reference to the plain tube probe.

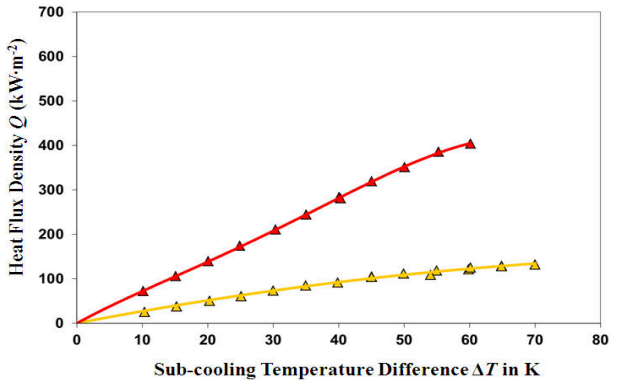

Fig. 12 Variation of heat flux density with sub-cooling temperature difference of drop condensation on meso- and mirco-scale profiled (▲) and plain tube (△).

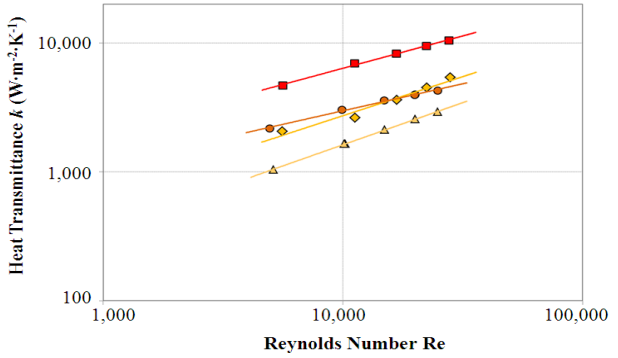

Fig. 13 Heat transmittance k and Reynolds number Re of the cooling fluid flow of (△) plain, (◇) meso-scale, (○) micro-scale, meso- and micro-scale profiled tube (□).

Comparative studies of the different probes at a sub-cooling temperature difference of ΔT = 60 K and a pressure of 1.1 bar were made by means of the heat transmittance k and the Reynolds number Re of the cooling fluid flow in the range of 5,000-25,000. On a double logarithmic scale, the slope of the function in any case appears to be of the type of a potential one, of which the measure of determination at least is larger than R^2 = 0.96. According to Eq. (9), the Reynolds number is proportional to the fluid velocity and the hydraulic diameter, while it is reciprocally proportional to the kinematic viscosity. Hence k is dominated significantly by the mass flow of the cooling fluid, both of the functions of the plain and the meso-scale profiled tube probes have an exponent value of $n \geq 0.6$, but that of the micro- and the combined meso- und micro-scale profiled ones showed a value of $n \leq 0.5$, wherefore the specific heat transmittance seems to be mass transport limited in the analyzed region.

4. Discussion

Because no microscopic analyzing devices were used during the experiments, microscopic and dynamic observations could not be made, for example, the distribution of homogeneous and heterogeneous condensation rates and cycles. Therefore, it became not clear whether the copper-water-steam-system occupies a Wenzel (wet) or a Cassie state, but from data referenced in literature, it could be the former one, wherefore further investigations would be necessary. These should include variations of the specific thermo-physical properties of the substrate and the fluid, probable nucleation site densities and very low sub-cooling temperature differences $\Delta T \leq 10$ K at a

higher resolution.

The absolute values of the heat transmittance, the heat flux density and the inner and outer heat transfer coefficients are in good agreement with those taken from the literature for copper and steel surfaces without promotors. In any case, these characteristic values increase significantly with the degree of sub-cooling temperature difference in the range of ΔT = 10-75 K and are a function of the Reynolds and the Prandtl number. The observed increase of the value of the contact angle implicates a decrease in the surface area covered by droplets, earlier fall-off and larger critical radius. The investigated inclinations of 45° and 90° resulted only in marginal variations of the values of the heat transmittance, the heat flux density and the heat transfer coefficient, wherefore with respect to the given substrates, it appears to be of second order.

Finally further analysis is preferable whether the observed limitation of the heat transmittance to a value of 11.4 $kW \cdot m^{-2} \cdot K^{-1}$ by mass transport could be eliminated by raising the mass flow of the cooling fluid up to a Reynolds number of Re = 100,000, whereby the heat transmittance is expected to increase remarkably to a value of k = 20 $kW \cdot m^{-2} \cdot K^{-1}$.

On balance, further investigations are desirable regarding special meso-, micro and even nano-scale profiled monolithic solids potentially with additional substantial coatings or artificially prepared compound substrates and textured composites. Thereby, the specific surface properties could be adjusted and the ability to induce enhanced condensation of a wide range of polar, non-polar and olefin substances in energy and process technology would be possible.

Acknowledgments

The authors thank Dr. Olga Böhme, Material Technology, Beuth University of Applied Sciences, Berlin, Germany, for electron scanning microscopy, the German Federal Ministry for Economic Affairs and Energy for grants by the Central Innovation Programme SME.

References

[1] S. Kabelac, VDI Heat Atlas, Verein Deutscher Ingenieure, 2nd ed., Hrsg, Springer, Berlin, Germany, 2010; pp. Jc1-Jc2.

[2] K. Stephan, Heat Transfer by Means of Condensation and Boiling, Wärmeübergang Beim Kondensieren und Beim Sieden, 1st ed., Springer, Berlin, Germany, 1988; pp. 6-25.

[3] H.F. Tekin, A theory of dropwise condensation, Master Thesis, Middle East Technical University, Ankara, Turkey, 2005.

[4] J. Boryenko, C. Chen, Self-propellent dropwise condensate on superhydrophobic surfaces, Physical Review Letters 103 (18) (2009) 184501-1-4.

[5] A. Tuteja, W. Choi, J. Mabry, G. McKinley, R. Cohen, Robust omniphobic surfaces, PNAS 105 (47) (2008) 18200-5.

[6] S. Khandekar, K. Muralidhar, Dropwise Condensation on Inclined Textured Surfaces, Springer Science and Business Media: New York, 2014; pp. 95-126.

[7] W. Kast, Theoretical and experimental investigation of heat transfer by means of drop condensation. VDI Improvement reports, Germany, Series 3, No. 6, 1965.

[8] T. Sun, G. Wang, L. Feng, B. Liu, Y. Ma, L. Jiang, et al., Reversible switching between superhydrophilicity and superhydrophobicity, Angewandte Chemie Int. Ed. 43 (3) (2004) 357-360.

[9] U. Hellwig, A. Kölling, M. Nowitzki, H. Sagasser, A. Schulz, A new type of nanostructured surface for chemical and renewable energy processing, in: Proc. Nanofair, Paper G8, Dresden, Germany, 2012, http://www.nanofair.com/en/review.html, (accessed February 3, 2015).

[10] C.E. Kirby, Promotion of dropwise condensation of ethyl alcohol, methyl alcohol and acetone by polytetrafluoroethylene, NASA TN D-6302, Washington D.C., 1971.

[11] A. Bisetto, D. Torresin, M.K. Tewari, D. Del Col, D. Poulikakos, Dropwise condensation on superhydrophobic nanostructured surfaces: Literature review and experimental analysis, Journal of Physics: Conference Series 501 (2014) 012028.

[12] L. Cheng, C.W.M. van der Geld, Experimental study of heat transfer and pressure drop characteristics of air/water and air-steam/water heat exchange in a polymer compact heat exchanger, Heat Transfer Engineering 26 (2) (2005) 18-27.

[13] D.W. Woodruff, J.W. Westwater, Steam condensation on various gold surfaces, Journal of Heat Transfer 103 (4)

(1981) 685-692.

[14] R. Enright, N. Miljkovic, J.L. Alvarado, K. Kim, J.W. Rose, Dropwise condensation on micro- and nanostructured surfaces, Nanoscale and Microscale Thermophysical Engineering 18 (3) (2014) 223-250.

[15] A.A. Karamalla, A.H. Yousif, B.M. Mohammed, Experimental analysis of heat transfer with dropwise and filmwise condensation on inclined double tubes heat exchanger, Engineering and Technology Journal Part (A) 32 (7) (2014) 1640-1654.

[16] H. Ohtake, Y. Kuizumi, S. Miyake, Study on Condensation Heat Transfer of Micro Structured Surfaces, in: ASME Proceedings Boiling and Condensation, 2009, pp. 49-52.

[17] S. Ravindran, Augmentation of condensation of water vapour: A review, Middle-East Journal of Scientific Research 20 (6) (2014) 770-776.

[18] M. Nahavandi, A. Mehrabani-Zeinabad, Effect of contact angle on steam dropwise condensation: A simulation approach, ISRN Chemical Engineering, 2012, 1-7, Article ID 789489.

[19] B.S. Sikarwar, N.K. Battoo, S. Kandekar, K. Muralidhar, Dropwise condensation underneath chemically textured surfaces: Simulation and experiments, Journal of Heat Transfer 133 (2011) 021501-1-021501-15.

[20] K. Rykaczewski, A.T. Paxson, M. Staymates, M.L. Walker, X. Sun, S. Anand, et al., Dropwise condensation of low surface tension fluids on omniphobic surfaces, Sci. Report 2014, 4, 4158, PMCID: PMC3942741, www.ncbi.nlm. nih.gov/pmc/articles/PMC3942741 (accessed: October 13, 2014).

[21] A. Schulz, G.N. Akapieva, V.V. Shirkovaa, H. Rösler, S.N. Dmitrieva, The overheat temperature for the boiling process on metallic surfaces with microstructured relief. Radiation Measurements 43 (2008) 612-616.

[22] S.G. Kandlikar, M.E. Steinke, Contact angles of droplets during spread and recoil after impinging on a heated surface, Trans IChemE: Part A 79 (2001) 491-498.

[23] R.N. Leach, F. Stevens, S.C. Langford, J.T. Dickinson, Experiments and simulations of nucleate and growth of water drops in a cooling system, Langmuir 22 (21) (2006) 8864-8872.

[24] A.D. Sommer, T.J. Best, K.F. Aid, Topography-based surface tension gradients to facilitate water droplet movement on laser-etched copper substrates, Langmuir 29 (2013) 12043-50.